Resting-state activity in development and maintenance of normal brain function

Carolyn E. Pizoli[a,1], Manish N. Shah[b,1], Abraham Z. Snyder[c,d], Joshua S. Shimony[d], David D. Limbrick[b], Marcus E. Raichle[c,d,e,f,1], Bradley L. Schlaggar[c,d,f,g], and Matthew D. Smyth[b]

[a]Department of Pediatrics, Duke University Medical Center, Durham, NC 27110; and Departments of [b]Neurological Surgery, [c]Neurology, [d]Radiology, [e]Biomedical Engineering, [f]Anatomy and Neurobiology, and [g]Pediatrics, Washington University School of Medicine, St. Louis, MO 63110

Contributed by Marcus E. Raichle, June 6, 2011 (sent for review March 1, 2011)

One of the most intriguing recent discoveries concerning brain function is that intrinsic neuronal activity manifests as spontaneous fluctuations of the blood oxygen level–dependent (BOLD) functional MRI signal. These BOLD fluctuations exhibit temporal synchrony within widely distributed brain regions known as resting-state networks. Resting-state networks are present in the waking state, during sleep, and under general anesthesia, suggesting that spontaneous neuronal activity plays a fundamental role in brain function. Despite its ubiquitous presence, the physiological role of correlated, spontaneous neuronal activity remains poorly understood. One hypothesis is that this activity is critical for the development of synaptic connections and maintenance of synaptic homeostasis. We had a unique opportunity to test this hypothesis in a 5-y-old boy with severe epileptic encephalopathy. The child developed marked neurologic dysfunction in association with a seizure disorder, resulting in a 1-y period of behavioral regression and progressive loss of developmental milestones. His EEG showed a markedly abnormal pattern of high-amplitude, disorganized slow activity with frequent generalized and multifocal epileptiform discharges. Resting-state functional connectivity MRI showed reduced BOLD fluctuations and a pervasive lack of normal connectivity. The child underwent successful corpus callosotomy surgery for treatment of drop seizures. Postoperatively, the patient's behavior returned to baseline, and he resumed development of new skills. The waking EEG revealed a normal background, and functional connectivity MRI demonstrated restoration of functional connectivity architecture. These results provide evidence that intrinsic, coherent neuronal signaling may be essential to the development and maintenance of the brain's functional organization.

developmental neuroimaging | epilepsy

It has been known since the advent of functional MRI (fMRI) that the blood oxygen level–dependent (BOLD) signal exhibits slow (nominally, <0.1 Hz) spontaneous fluctuations (1). These fluctuations were initially regarded as noise in the context of task-related fMRI. However, in 1995 it was shown that these fluctuations are temporally coherent within widely distributed regions that recapitulate the topography of fMRI responses induced by performance of typical sensory, motor, and cognitive tasks (2, 3). This phenomenon is known as functional connectivity. Because functional connectivity is most easily demonstrated in quietly resting humans, the associated spatial topographies are now widely known as resting-state networks (RSNs) (3–5).

RSNs have been demonstrated in all animal species examined so far (6–8). They are present in rudimentary form early in human life (9–11) and later reorganize as brain development proceeds through childhood (12–15). RSNs persist, albeit in somewhat modified form, during task performance (16), sleep (17, 18), and even under sedation (7, 19, 20). Thus, RSNs normally represent a remarkably robust phenomenon.

Little is known about the physiological functions represented by RSNs, however. The available evidence suggests that RSNs reflect slow, synchronous, spontaneous fluctuations of spatially organized neural signaling (21–24). This signaling is energetically expensive (25, 26), implying that it must serve critical functions. It has been suggested, in very broad terms, that these functions maintain the brain's integrity and increase its capacity to deal effectively with future exigencies (26–28); however, this perspective remains entirely theoretical. In addition to maintaining network integrity, the spontaneous neuronal signaling represented by RSNs also may be involved in the construction or development of neural networks (9, 29, 30). This case report provides evidence supporting the view that RSNs represent physiological processes critical to the development and maintenance of the brain's functional integrity.

Case Report

The patient is a 5-y-old boy with epileptic encephalopathy (EE) presenting as frequent mixed seizure types, characteristic EEG abnormalities, and developmental regression, collectively known as Lennox–Gastaut syndrome (LGS) (31). Birth was complicated by twin gestation and delivery at 35 wk gestational age. The neonatal course was uncomplicated, and early development was notable only for mild expressive speech delay. Atypical absence, atonic drop, and generalized tonic-clonic seizures began around age 4 y. Over the next year, the frequency of drop seizures increased progressively (to 5–20/d), accompanied by regression of language skills, toilet training, and social behavior. Multiple courses of antiepileptic drugs failed to control the seizures. Neuropsychological testing with a combination of child tests and parent questionnaires (32–34) revealed abnormal behavior. Structural MRI findings were normal (Fig. 1*A*). EEG was markedly abnormal, with absence of an age-appropriate posterior dominant rhythm (35, 36), variable amplitude delta/theta slowing, frequent generalized slow (2–3 Hz) spike-and-wave discharges, and multifocal spikes (Fig. 1*C*).

After evaluation by the multidisciplinary epilepsy team, the patient underwent anterior two-thirds corpus callosotomy for treatment of drop attacks (Fig. 1*B*). There were no complications. Postoperatively, there was a nearly complete remission of all seizure types (37, 38). Remarkably, cognitive development resumed in all areas, including language skills, toilet training, and social behavior. EEG recorded at 4 mo after surgery showed striking improvement; an age-appropriate continuous 8-Hz posterior dominant rhythm was present, and the disorganized background slowing was completely resolved (Fig. 1*D*). At 6 mo, formal neuropsychological testing revealed little change relative to the preoperative baseline, but at school, the patient was able to function in a mainstream classroom on a half-day basis.

Author contributions: A.Z.S., M.E.R., B.L.S., and M.D.S. designed research; C.E.P., M.N.S., A.Z.S., J.S.S., D.D.L., M.E.R., B.L.S., and M.D.S. performed research; C.E.P., M.N.S., A.Z.S., and J.S.S. contributed new reagents/analytic tools; C.E.P., M.N.S., A.Z.S., and J.S.S. analyzed data; and C.E.P., M.N.S., A.Z.S., J.S.S., M.E.R., B.L.S., M.D.S. wrote the paper; and D.D.L. performed the callosotomy and treated the patient.

The authors declare no conflict of interest.

Freely available online through the PNAS open access option.

[1]C.E.P. and M.N.S. contributed equally to this work.

[2]To whom correspondence may be addressed. E-mail: shahma@wudosis.wustl.edu or marc@npg.wustl.edu.

This article contains supporting information online at www.pnas.org/lookup/suppl/doi:10.1073/pnas.1109144108/-/DCSupplemental.

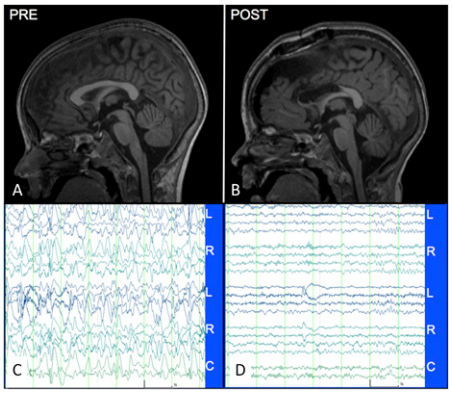

Fig. 1. Structural MRI (midline sagittal T1-weighted MP-RAGE) and EEG. (*A*) Preoperative MRI shows normal structure. (*B*) Postoperative MRI (on postoperative day 1) shows the extent of the anterior two-thirds corpus callosotomy. Widening of the interhemispheric fissure, a common postoperative finding, also is evident. (*C*) Waking EEG (10 μV/mm, 1 s spacing) recorded 6 mo preoperatively using a standard ("double banana") bipolar montage. The record is severely abnormal (see text). (*D*) Normal waking EEG recorded 4 mo postoperatively. "L," "R," and "C" denote left, right, and central derivations. The montage, time, and amplitude scales are identical in *C* and *D*.

Results

Seed-Based Functional Connectivity. The preoperative correlation maps corresponding to all seed regions were largely devoid of recognizable RSN architecture and instead were dominated by features attributable to correlated noise in blood vessels, white matter, and cerebrospinal fluid (CSF) (Fig. 2, *Middle*). Postoperatively, the correlation maps differed dramatically, with features predominantly in gray matter with age-appropriate structure evident in multiple RSNs (Fig. 2, *Right*); see *SI Text* for additional illustrative results, including postoperative restoration of normal RSN architecture within the default mode network. Comparable preoperative vs. postoperative functional connectivity MRI (fcMRI) results also were obtained using spatial independent component analysis (30 components). Homotopic functional connectivity in the postoperative results (i.e., right hemisphere correlations contralateral to left hemisphere seeds) was variable and a clear result of the corpus callosotomy (Fig. 2).

BOLD Signal Fluctuation Variance. The remarkable postoperative improvement in functional connectivity raised the question of whether the preoperative findings were attributable to an excess of noise or to a lack of signal. To investigate this question, we examined BOLD signal SDs at the level of both voxels and regions of interest (ROIs). The preoperative SD maps showed signal variance predominantly in CSF and vascular spaces (Fig. 3*A*); in contrast, the postoperative SD map showed BOLD signal fluctuations mostly in gray matter (Fig. 3*B*). Quantitative results were obtained for the 46 canonical ROIs listed in *SI Text* (all in gray matter). The preoperative BOLD signal SD averaged over all ROIs was less than the postoperative value by a factor of ~2 (*SI Text*). Thus, the preoperative RSN abnormalities can be interpreted as a lack of signal rather than an excess of noise.

Pairwise ROI–ROI Correlations and Covariances. Preoperative and postoperative BOLD signal ROI pair correlation and covariance matrices are shown in Fig. 4. The ROIs are ordered according to functional system (*SI Text*) to facilitate visualization of coherent, spontaneous BOLD fluctuations within RSNs. Coherent resting-state BOLD fluctuations within and across functional systems are evident in the block structure of the postoperative results (Fig. 4). The preoperative results are much less well organized. Importantly, the preoperative vs. postoperative change in functional connectivity is most apparent in Fig. 4 *C* and *D*, which shows ROI–ROI covariance. Unlike correlation, covariance reflects

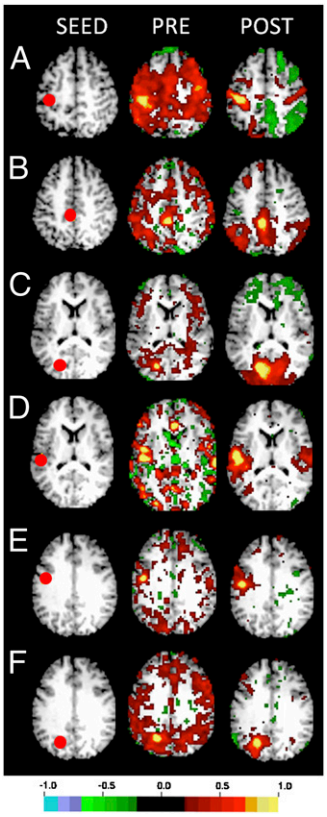

Fig. 2. Selected seed-based correlation maps. Columns show the seeds (*Left*), preoperative maps (*Middle*), and postoperative maps (*Right*). The map quantity illustrated is the Fisher *z*-transformed correlation coefficient thresholded at ± 0.2. (*A*) Left somatomotor cortex seed (−39 −26 51); somatomotor RSN. (*B*) Left posterior cingulate/precuneus seed (−4 −40 43); default mode network (DMN). (*C*) Visual cortex seed (−20 −75 12). (*D*) Auditory cortex seed (−50 −25 8). (*E*) Left inferior frontal gyrus seed (−48 −13 31); speech. (*F*) Left intraparietal sulcus seed (−24 −69 30); dorsal attention network. Note the marked improvement in RSN organization in the postoperative maps vs. the preoperative maps.

signal pair magnitudes as well as temporal coherence (*SI Text*, *Mathematical Note*). Comparison of Fig. 4 *A–C* versus *B–D* illustrates the fundamental fMRI findings in this case, specifically reversibly suppressed spontaneous BOLD fluctuations; this effect is most evident along the matrix diagonals in *C* and *D*.

Discussion

EEG and fMRI in the Study of Childhood-Onset EE. EE is a large umbrella category of childhood epilepsy that includes many distinct clinical entities, such as West syndrome and LGS, that themselves may be secondary to a variety of pathophysiologies (39). Suppression of BOLD RSNs is not recognized as a constant or even common feature of EE. There have been few fMRI studies in this patient population. Three previous studies were based on simultaneous EEG and fMRI recordings without investigation of resting-state functional connectivity (40–42). One study of very young children with hypsarrythmia found predominantly positive BOLD responses to EEG epileptiform events and delta range slowing with highly variable localization (42). In contrast, predominantly negative BOLD responses in regions within the default mode network were observed during bilaterally synchronous EEG spikes in children with continuous spikes and waves during slow sleep (40, 41).

Although there is no characteristic EEG feature of EE that is most closely associated with clinical disability (43), there is general agreement that early successful medical or surgical treat-

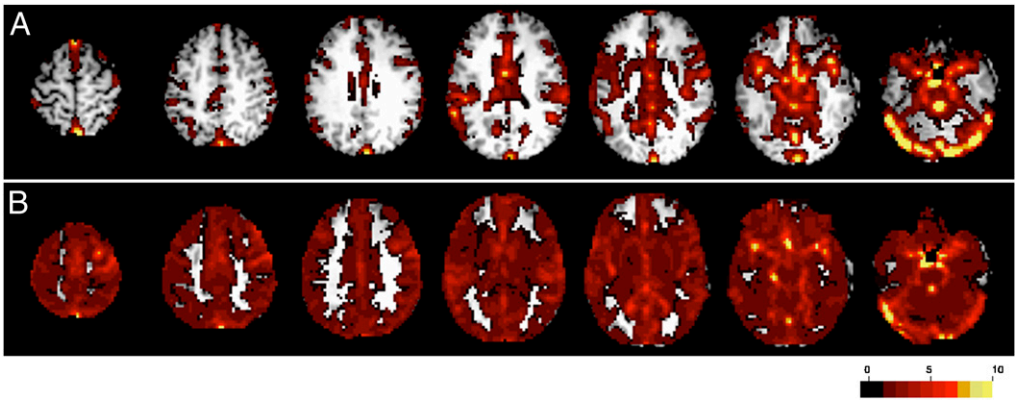

Fig. 3. Voxel-wise SD maps. (*A*) Preoperative results. High signal variation is seen primarily in vascular and CSF spaces. (*B*) Postoperative results. High signal variation is seen primarily in gray matter.

ment is associated with improved developmental outcome (44–47); see *SI Text* for more discussion of this. Thus, EE appears to be injurious, but the mechanism of injury remains uncertain.

Effects of Corpus Callosotomy on Resting-State Functional Connectivity. The corpus callosum is largely responsible for spread of seizures across the midline (48). Anterior callosotomy is performed to sever connections supporting seizure generalization while conserving posterior fibers that carry perceptual information. Previously reported postcallosotomy EEG changes include improved background organization and reduced bisynchronous epileptiform discharges (49), as seen in our patient.

We previously described resting-state functional connectivity in a 6-y-old child with atonic-myoclonic epilepsy who underwent complete callosotomy, with the main point of that report being the nearly complete loss of interhemispheric functional connectivity in the immediate postoperative period (50). That child differed from the current patient in several respects, with less severe preoperative EEG abnormalities (presence of a 7-Hz posterior dominant rhythm and lack of epileptiform activity in the waking record) and preoperative fMRI showing normal RSNs. In contrast, Uddin et al. (51) described essentially normal interhemispheric functional connectivity in a 74-y-old woman with a remote history (more than 4 decades antecedent) of complete callosotomy. The variable extent of postoperative interhemispheric functional connectivity in our patient most likely reflects preservation of the posterior third of the corpus callosum. However, we note that the intraparietal sulcus regions did not show homotopic functional connectivity (Fig. 2*F*), even though the callosal connections of these regions likely were spared. All of these callosotomy cases underscore the point that the relationship between anatomic (axonal) connectivity and functional connectivity (BOLD signal correlation) is complicated, as well as subject to change over time (7, 52–57).

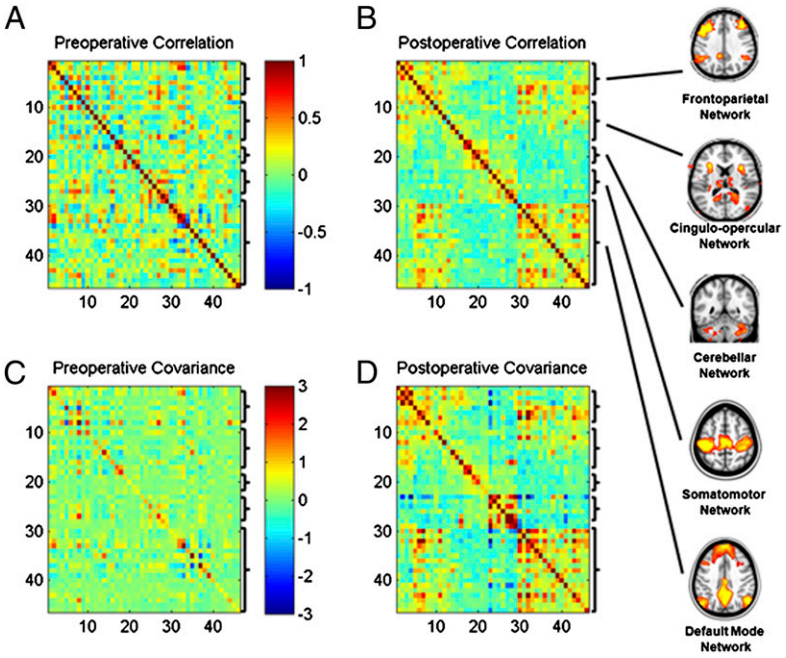

Fig. 4. Correlation and covariance matrices corresponding to 46 ROIs taken pairwise. The ROIs are ordered according to functional networks delineated by brackets and depicted on the right; see *SI Text* for details. (*A*) Preoperative correlation. (*B*) Postoperative correlation. (*C*) Preoperative covariance. (*D*) Postoperative covariance. Note the improved RSN organization evident in the block structure of the postoperative results, especially comparing *C* and *D*. The diagonals in *D* and *B* show a pronounced postoperative increase in BOLD signal variance.

Suppressed Resting-State Activity. A major finding in the present case is the association of EE, including archetypical clinical and electroencephalographic features, with suppressed spontaneous BOLD fluctuations. Thus, it appears that resting-state BOLD fluctuations of insufficient magnitude may constitute an abnormality. Data defining the range of normal magnitudes in this clinical population are scanty. To evaluate the degree of abnormality in the present case, we computed resting-state regional BOLD signal SDs in a cohort of comparable neurosurgical patients using the same 46 ROIs illustrated in Fig. 4. Our patient's preoperative resting-state BOLD mean SD was lower than that of all patients in the comparison cohort (70 datasets acquired in 43 patients) (*SI Text*). Postoperatively, the patient's mean SD was at the lower end of the range in the comparison cohort.

Several groups have reported focally reduced amplitude of low-frequency BOLD fluctuations in various neuropsychiatric conditions (54, 58, 59). It is highly likely that these effects are related to the RSN changes associated with many degenerative and psychiatric diseases (for reviews see refs. 60–62). Unlike in the present case, previously reported amplitudes of low-frequency BOLD fluctuation effects were focal and often verged on statistical significance. To the best of our knowledge, the observation of globally suppressed spontaneous BOLD fluctuations is novel.

The degree to which suppression of BOLD RSNs corresponds to clinical severity in EE, and more specifically to behavioral regression, is an important question. ^{18}F-fluorodeoxyglucose (FDG)-PET measurements of the cerebral metabolic rate of glucose (CMRglu) are pertinent to this question. Specifically, Chugani and coworkers (63, 64) defined four categories of LGS according to the level of suppressed glucose metabolism in a small cohort of these patients. Almost all of the patients had some degree of cognitive impairment, but a normal CMRglu was correlated with better intellectual function. The authors found no correlation between local CMRglu and duration or frequency of seizures. Other studies have suggested that static encephalopathy in this population may correlate with reduced CMRglu (65, 66). FDG-PET studies have indicated that glucose hypometabolism (focal as well as global) generally reverses after successful treatment of EE (66, 67), which is parallel to the present case. It is important to recognize that glucose metabolism is central to numerous processes apart from energy production that are linked to cellular survival (68). Thus, depressed CMRglu can be directly related to disrupted development in children with EE.

In our present data, the amplitude of resting-state BOLD fluctuations, as assessed by the SD measure, was lower in the children who underwent callosotomy, all of whom had drop seizures (a correlate of which is cognitive impairment), compared with patients with other conditions, including temporal lobe epilepsy and focal dysplasia (*SI Text*). There exist suggestive data supporting the notion that suppressed resting-state activity correlates with behavioral impairment. Investigating this question is difficult because sedation, which almost invariably must be administered to enable measurement, itself has an effect on measured BOLD SD (*SI Text*). Moreover, some patients with EE have preexisting static impairments, such as cerebral palsy and structural abnormalities, that complicate the question of what can be attributed to suppressed brain activity in these cases. But this complication does not apply in the present case, given that the child was clinically nearly normal until the onset of LGS.

Implications Related to the Physiological Significance of Resting-State BOLD Fluctuations. RSNs are plastic and reorganize in response to altered sensory input, as in early-onset blindness secondary to retinal injury (69). RSNs reorganize after vascular brain injury in parallel with recovery of function (70). In normal volunteers, RSNs can be manipulated experimentally by intensive perceptual training or simply by recent performance of cognitive tasks (71, 72). These results demonstrate that RSNs are sculpted by experience and are consistent with the notion that ongoing neuronal activity plays a role in recovery of function after injury; however, they fall short of demonstrating that resting-state activity plays a central role in maintaining normal brain function. It is precisely this point on which the significance of the present case rests. The key observation in this case is the association of suspended normal development with suppression of BOLD fluctuations and reversal of both abnormalities after treatment. The implication is that ongoing, temporally coherent neuronal signaling may play a role in maintaining the brain's functional integrity.

It is well established that temporally coherent spontaneous neuronal activity plays a critical role in shaping synaptic weights during brain development (69, 73, 74). Moreover, it is known that some of the mechanisms regulating synaptic strength in relation to neuronal activity during development persist into adulthood (75). Such results derive from studies currently classified under the heading of activity-dependent synaptic homeostasis (76). Much of the synaptic homeostasis literature is based on experiments conducted in vitro or in small animals and is focused on the cellular and molecular mechanisms underlying synaptic plasticity. This area of inquiry may seem far removed from EE. However, our present findings suggest that disordered activity-dependent synaptic homeostasis may well underlie the pathophysiology of EE. Improved understanding of EE as a disease entity could aid the development of a suitable animal model that can illuminate the molecular mechanisms that normally maintain the brain's development and functional integrity. However, as far as we know, no such animal model exists, and thus there is a need to identify more patients with EE to further clarify the importance of spontaneous BOLD fluctuations and their correlation with neurobiological development.

Limitations, Unresolved Issues, and Future Directions. Caution is appropriate when interpreting the findings for any individual patient. Several limitations of the present study can be identified, as follows:

- Because of the history of mixed seizures, the patient was maintained on antiepileptic drugs postoperatively. Antiepileptic drugs can affect cognition (reviewed in ref. 77) and cerebral glucose metabolism (78). However, the same antiepileptic drug regimen was maintained over the preoperative and postoperative fcMRI acquisition period, and thus this factor does not account for the patient's clinical course.
- All fMRI images were acquired with the patient under propofol sedation, which is known to affect RSN topography (79). However, a detailed analysis including comparable neurosurgical epilepsy patients (*SI Text*) demonstrated that sedation alone does not account for the present principal findings.
- Our observations are essentially correlative. We report the associations of suppressed coherent resting-state BOLD fluctuations with seizures, developmental regression, and characteristic EEG abnormalities (LGS). Critically, these associations were reversed, albeit incompletely, after successful treatment. The FDG-PET literature suggests that preoperatively depressed CMRglu, had it been measured, also would have been restored postoperatively. The patient's postoperative clinical improvement cannot be attributed to any of these factors in isolation; rather, our data suggest that RSN activity may play a heretofore underrecognized role in maintaining the brain's functional integrity.
- Nature provides very few opportunities to observe the behavioral and EEG correlates of reversibly suppressed resting-state BOLD fluctuations. In view of this, we intend to create a prospective registry for imaging these children and following them before and after intervention to study the relationships among resting-state activity, behavior, and development.

Methods

Data Acquisition. Brain MRI (Siemens 3-T TRIO scanner) was performed 1 d before and 1 d after the surgery with the patient on a constant antiepileptic drug regimen. Resting-state BOLD fMRI was added to the clinical protocol after signed informed consent was obtained from the patient's parents in accordance with institutional review board standards. Because of the patient's age and developmental level, all imaging was obtained under propofol sedation (*SI Text*). Structural imaging included a high-resolution, T1-weighted, magnetization-prepared gradient echo (MP-RAGE) scan and a T2-weighted fast-spin echo scan. Functional data were acquired using a gradient echo, echo-planar sequence sensitive to BOLD contrast (repetition time, 2.07 s; echo time, 25 ms; flip angle, 90°; bandwidth, 2605 Hz; two runs of 7 min each). Whole-brain coverage was obtained in 36 contiguous slices (4 mm cubic voxels). Head motion was minimal in both the preoperative and postoperative fMRI datasets.

Preprocessing of fMRI Data. The fMRI data were preprocessed as described previously (50, 80). Preprocessing steps included compensation for asynchronous slice acquisition and head motion within and across fMRI runs. Intensity scaling (one multiplicative factor per fMRI run applied to all voxels and all volumes) was used to obtain a whole-brain mode value of 1,000. Registration of the functional data to Talairach atlas space (81) was computed using the patient's T1- and T2-weighted structural images and an atlas-representative template prepared from MP-RAGE images acquired in 24 normal children and young adults; the template generation methodology was described previously (82). Additional preparation of the fMRI data for correlation analysis included temporal low-pass filtering retaining frequencies below 0.1 Hz and spatial smoothing (6 mm FWHM Gaussian blur). Spurious variance was reduced by regression of the six head motion parameters, the time series derived from ventricular and white matter regions, and the signal averaged over the whole brain (80).

Correlation Analysis. Forty-six 10-mm-diameter spherical seed regions (ROIs; *SI Text*) were centered on coordinates associated with task control (83), attention (84), and default mode functionality (85), along with additional foci in primary sensory and motor areas. BOLD time series were extracted from each seed ROI. Correlation maps were computed using standard methods (80). Obtained correlation coefficients were transformed using Fisher's variance-stabilizing *z*-transform. ROI pair covariances and correlations were computed similarly. Independent component analysis was performed using a modified fast independent component analysis (ICA) algorithm implemented in MATLAB (86).

ACKNOWLEDGMENTS. We thank Dongyang Zhang for implementing the fast ICA algorithm, Mike Morrissey for assisting with the EEG record, Judy Weisenberg for managing the patient's epilepsy, and Jeff Titus for providing a neuropsychological assessment of the patient. This work was supported by Neurological Sciences Academic Development Award NS001690 (to C.E.P. and B.L.S.) and National Institutes of Health Grants T32 NS007205 (to M.N.S.), K23-HD053212 (to J.S.S.), NS053425 (to B.L.S.), P30NS048056 (to A.Z.S.), and P30NS06833 (to M.E.R. and A.Z.S.).

1. Purdon PL, Weisskoff RM (1998) Effect of temporal autocorrelation due to physiological noise and stimulus paradigm on voxel-level false-positive rates in fMRI. *Hum Brain Mapp* 6:239–249.
2. Biswal B, Yetkin FZ, Haughton VM, Hyde JS (1995) Functional connectivity in the motor cortex of resting human brain using echo-planar MRI. *Magn Reson Med* 34: 537–541.
3. Smith SM, et al. (2009) Correspondence of the brain's functional architecture during activation and rest. *Proc Natl Acad Sci USA* 106:13040–13045.
4. Cole DM, Smith SM, Beckmann CF (2010) Advances and pitfalls in the analysis and interpretation of resting-state FMRI data. *Front Syst Neurosci* 4:8.
5. Biswal BB, et al. (2010) Toward discovery science of human brain function. *Proc Natl Acad Sci USA* 107:4734–4739.
6. Pawela CP, et al. (2008) Resting-state functional connectivity of the rat brain. *Magn Reson Med* 59:1021–1029.
7. Vincent JL, et al. (2007) Intrinsic functional architecture in the anaesthetized monkey brain. *Nature* 447:83–86.
8. van Meer MP, et al. (2010) Recovery of sensorimotor function after experimental stroke correlates with restoration of resting-state interhemispheric functional connectivity. *J Neurosci* 30:3964–3972.
9. Doria V, et al. (2010) Emergence of resting state networks in the preterm human brain. *Proc Natl Acad Sci USA* 107:20015–20020.
10. Gao W, et al. (2009) Evidence on the emergence of the brain's default network from 2-week-old to 2-year-old healthy pediatric subjects. *Proc Natl Acad Sci USA* 106: 6790–6795.
11. Smyser CD, et al. (2010) Longitudinal analysis of neural network development in preterm infants. *Cereb Cortex* 20:2852–2862.
12. Fair DA, et al. (2010) Maturing thalamocortical functional connectivity across development. *Front Syst Neurosci* 4:10.
13. Fair DA, et al. (2007) Development of distinct control networks through segregation and integration. *Proc Natl Acad Sci USA* 104:13507–13512.
14. Fransson P, et al. (2007) Resting-state networks in the infant brain. *Proc Natl Acad Sci USA* 104:15531–15536.
15. Fransson P, Aden U, Blennow M, Lagercrantz H (2011) The functional architecture of the infant brain as revealed by resting-state fMRI. *Cereb Cortex* 21:145–154.
16. Fransson P (2006) How default is the default mode of brain function? Further evidence from intrinsic BOLD signal fluctuations. *Neuropsychologia* 44:2836–2845.
17. Horovitz SG, et al. (2009) Decoupling of the brain's default mode network during deep sleep. *Proc Natl Acad Sci USA* 106:11376–11381.
18. Larson-Prior LJ, et al. (2009) Cortical network functional connectivity in the descent to sleep. *Proc Natl Acad Sci USA* 106:4489–4494.
19. Greicius MD, et al. (2008) Persistent default-mode network connectivity during light sedation. *Hum Brain Mapp* 29:839–847.
20. Stamatakis EA, Adapa RM, Absalom AR, Menon DK (2010) Changes in resting neural connectivity during propofol sedation. *PLoS ONE* 5:e14224.
21. Shmuel A, Leopold DA (2008) Neuronal correlates of spontaneous fluctuations in fMRI signals in monkey visual cortex: Implications for functional connectivity at rest. *Hum Brain Mapp* 29:751–761.
22. Nir Y, et al. (2008) Interhemispheric correlations of slow spontaneous neuronal fluctuations revealed in human sensory cortex. *Nat Neurosci* 11:1100–1108.
23. He BJ, Snyder AZ, Zempel JM, Smyth MD, Raichle ME (2008) Electrophysiological correlates of the brain's intrinsic large-scale functional architecture. *Proc Natl Acad Sci USA* 105:16039–16044.
24. Wu CW, et al. (2009) Mapping functional connectivity based on synchronized CMRO2 fluctuations during the resting state. *Neuroimage* 45:694–701.
25. Raichle ME, Mintun MA (2006) Brain work and brain imaging. *Annu Rev Neurosci* 29: 449–476.
26. Raichle ME (2010) Two views of brain function. *Trends Cogn Sci* 14:180–190.
27. Miall RC, Robertson EM (2006) Functional imaging: Is the resting brain resting? *Curr Biol* 16:R998–R1000.
28. Uddin LQ, Supekar K, Menon V (2010) Typical and atypical development of functional human brain networks: Insights from resting-state fMRI. *Front Syst Neurosci* 4:21.
29. Supekar K, et al. (2010) Development of functional and structural connectivity within the default mode network in young children. *Neuroimage* 52:290–301.
30. Zielinski BA, Gennatas ED, Zhou J, Seeley WW (2010) Network-level structural covariance in the developing brain. *Proc Natl Acad Sci USA* 107:18191–18196.
31. Heiskala H (1997) Community-based study of Lennox–Gastaut syndrome. *Epilepsia* 38: 526–531.
32. Doyle A, Ostrander R, Skare S, Crosby RD, August GJ (1997) Convergent and criterion-related validity of the Behavior Assessment System for Children-Parent Rating Scale. *J Clin Child Psychol* 26:276–284.
33. Gottfried AW, Guerin D, Spencer JE, Meyer C (1984) Validity of Minnesota Child Development Inventory in screening young children's developmental status. *J Pediatr Psychol* 9:219–230.
34. Wei Y, Oakland T, Algina J (2008) Multigroup confirmatory factor analysis for the Adaptive Behavior Assessment System II parent form, ages 5–21. *Am J Ment Retard* 113:178–186.
35. Grigg-Damberger M, et al. (2007) The visual scoring of sleep and arousal in infants and children. *J Clin Sleep Med* 3:201–240.
36. Petersén I, Eeg-Olofsson O (1971) The development of the electroencephalogram in normal children from the age of 1 through 15 years: Non-paroxysmal activity. *Neuropadiatrie* 2:247–304.
37. Jalilian L, et al. (2010) Complete vs. anterior two-thirds corpus callosotomy in children: Analysis of outcome. *J Neurosurg Pediatr* 6:257–266.
38. Shimizu H (2005) Our experience with pediatric epilepsy surgery focusing on corpus callosotomy and hemispherotomy. *Epilepsia* 46(Suppl 1):30–31.
39. Dulac O (2001) Epileptic encephalopathy. *Epilepsia* 42(Suppl 3):23–26.
40. De Tiège X, et al. (2007) Impact of interictal epileptic activity on normal brain function in epileptic encephalopathy: An electroencephalography-functional magnetic resonance imaging study. *Epilepsy Behav* 11:460–465.
41. Siniatchkin M, et al. (2010) Neuronal networks in children with continuous spikes and waves during slow sleep. *Brain* 133:2798–2813.
42. Siniatchkin M, et al. (2007) Different neuronal networks are associated with spikes and slow activity in hypsarrhythmia. *Epilepsia* 48:2312–2321.
43. Lux AL (2007) Is hypsarrhythmia a form of non-convulsive status epilepticus in infants? *Acta Neurol Scand* 115(4, Suppl):37–44.
44. Asarnow RF, et al. (1997) Developmental outcomes in children receiving resection surgery for medically intractable infantile spasms. *Dev Med Child Neurol* 39:430–440.
45. Freitag H, Tuxhorn I (2005) Cognitive function in preschool children after epilepsy surgery: Rationale for early intervention. *Epilepsia* 46:561–567.
46. Kivity S, et al. (2004) Long-term cognitive outcomes of a cohort of children with cryptogenic infantile spasms treated with high-dose adrenocorticotropic hormone. *Epilepsia* 45:255–262.
47. Matsuzaka T, et al. (2001) Developmental assessment–based surgical intervention for intractable epilepsies in infants and young children. *Epilepsia* 42(Suppl 6):9–12.
48. Asadi-Pooya AA, Sharan A, Nei M, Sperling MR (2008) Corpus callosotomy. *Epilepsy Behav* 13:271–278.
49. Quattrini A, et al. (1997) EEG patterns after callosotomy. *J Neurosurg Sci* 41:85–92.

50. Johnston JM, et al. (2008) Loss of resting interhemispheric functional connectivity after complete section of the corpus callosum. *J Neurosci* 28:6453–6458.
51. Uddin LQ, et al. (2008) Residual functional connectivity in the split-brain revealed with resting-state functional MRI. *Neuroreport* 19:703–709.
52. Barnes KA, et al. (2010) Identifying basal ganglia divisions in individuals using resting-state functional connectivity MRI. *Front Syst Neurosci* 4:18.
53. Di Martino A, et al. (2008) Functional connectivity of human striatum: A resting state FMRI study. *Cereb Cortex* 18:2735–2747.
54. Zhang D, et al. (2008) Intrinsic functional relations between human cerebral cortex and thalamus. *J Neurophysiol* 100:1740–1748.
55. Krienen FM, Buckner RL (2009) Segregated fronto-cerebellar circuits revealed by intrinsic functional connectivity. *Cereb Cortex* 19:2485–2497.
56. Damoiseaux JS, Greicius MD (2009) Greater than the sum of its parts: A review of studies combining structural connectivity and resting-state functional connectivity. *Brain Struct Funct* 213:525–533.
57. Dosenbach NU, Fair DA, Cohen AL, Schlaggar BL, Petersen SE (2008) A dual-networks architecture of top-down control. *Trends Cogn Sci* 12:99–105.
58. Hoptman MJ, et al. (2010) Amplitude of low-frequency oscillations in schizophrenia: a resting state fMRI study. *Schizophr Res* 117:13–20.
59. Seeley WW, Crawford RK, Zhou J, Miller BL, Greicius MD (2009) Neurodegenerative diseases target large-scale human brain networks. *Neuron* 62:42–52.
60. Fox MD, Greicius M (2010) Clinical applications of resting state functional connectivity. *Front Syst Neurosci* 4:19.
61. Zhang D, Raichle ME (2010) Disease and the brain's dark energy. *Nat Rev Neurol* 6: 15–28.
62. Zhou J, et al. (2010) Divergent network connectivity changes in behavioural variant frontotemporal dementia and Alzheimer's disease. *Brain* 133:1352–1367.
63. Chugani HT (1994) The role of PET in childhood epilepsy. *J Child Neurol* 9(Suppl 1): S82–S88.
64. Chugani HT, Mazziotta JC, Engel J, Jr., Phelps ME (1987) The Lennox–Gastaut syndrome: Metabolic subtypes determined by 2-deoxy-2[18F]fluoro-D-glucose positron emission tomography. *Ann Neurol* 21:4–13.
65. Theodore WH, et al. (1987) Cerebral glucose metabolism in the Lennox–Gastaut syndrome. *Ann Neurol* 21:14–21.
66. Metsähonkala L, et al. (2002) Focal and global cortical hypometabolism in patients with newly diagnosed infantile spasms. *Neurology* 58:1646–1651.
67. Itomi K, et al. (2002) Prognostic value of positron emission tomography in cryptogenic West syndrome. *Dev Med Child Neurol* 44:107–111.
68. Vander Heiden MG, Cantley LC, Thompson CB (2009) Understanding the Warburg effect: The metabolic requirements of cell proliferation. *Science* 324:1029–1033.
69. Liu Y, et al. (2007) Whole brain functional connectivity in the early blind. *Brain* 130: 2085–2096.
70. Wang L, et al. (2010) Dynamic functional reorganization of the motor execution network after stroke. *Brain* 133:1224–1238.
71. Lewis CM, Baldassarre A, Committeri G, Romani GL, Corbetta M (2009) Learning sculpts the spontaneous activity of the resting human brain. *Proc Natl Acad Sci USA* 106:17558–17563.
72. Stevens WD, Buckner RL, Schacter DL (2009) Correlated low-frequency BOLD fluctuations in the resting human brain are modulated by recent experience in category-preferential visual regions. *Cereb Cortex* 20:1997–2006.
73. Katz LC, Shatz CJ (1996) Synaptic activity and the construction of cortical circuits. *Science* 274:1133–1138.
74. Shah RD, Crair MC (2008) Mechanisms of response homeostasis during retinocollicular map formation. *J Physiol* 586:4363–4369.
75. Maffei A, Fontanini A (2009) Network homeostasis: A matter of coordination. *Curr Opin Neurobiol* 19:168–173.
76. Turrigiano GG, Nelson SB (2004) Homeostatic plasticity in the developing nervous system. *Nat Rev Neurosci* 5:97–107.
77. Marsh ED, Brooks-Kayal AR, Porter BE (2006) Seizures and antiepileptic drugs: Does exposure alter normal brain development? *Epilepsia* 47:1999–2010.
78. Theodore WH (1988) Antiepileptic drugs and cerebral glucose metabolism. *Epilepsia* 29(Suppl 2):S48–S55.
79. Mhuircheartaigh RN, et al. (2010) Cortical and subcortical connectivity changes during decreasing levels of consciousness in humans: A functional magnetic resonance imaging study using propofol. *J Neurosci* 30:9095–9102.
80. Fox MD, Zhang D, Snyder AZ, Raichle ME (2009) The global signal and observed anticorrelated resting state brain networks. *J Neurophysiol* 101:3270–3283.
81. Lancaster JL, et al. (1995) A modality-independent approach to spatial normalization of tomographic images of the human brain. *Hum Brain Mapp* 3:209–223.
82. Buckner RL, et al. (2004) A unified approach for morphometric and functional data analysis in young, old, and demented adults using automated atlas-based head size normalization: Reliability and validation against manual measurement of total intracranial volume. *Neuroimage* 23:724–738.
83. Dosenbach NU, et al. (2006) A core system for the implementation of task sets. *Neuron* 50:799–812.
84. Fox MD, Corbetta M, Snyder AZ, Vincent JL, Raichle ME (2006) Spontaneous neuronal activity distinguishes human dorsal and ventral attention systems. *Proc Natl Acad Sci USA* 103:10046–10051.
85. Fox MD, et al. (2005) The human brain is intrinsically organized into dynamic, anticorrelated functional networks. *Proc Natl Acad Sci USA* 102:9673–9678.
86. Hyvärinen A (1999) Fast and robust fixed-point algorithms for independent component analysis. *IEEE Trans Neural Netw* 10:626–634.